Exclusive production of ϕ meson in the $\gamma^* p \to \phi p$ reaction at large photon virtualities within k_T-factorization approach

A. D. Bolognino,[1,2,*] A. Szczurek,[3,4,†] and W. Schäfer[4,‡]

[1]*Dipartimento di Fisica, Università della Calabria, I-87036 Arcavacata di Rende, Cosenza, Italy*
[2]*Istituto Nazionale di Fisica Nucleare, Gruppo collegato di Cosenza, I-87036 Arcavacata di Rende, Cosenza, Italy*
[3]*College of Natural Sciences, Institute of Physics, University of Rzeszów, ul. Pigonia 1, PL-35-310 Rzeszów, Poland*
[4]*Institute of Nuclear Physics, Polish Academy of Sciences, ul. Radzikowskiego 152, PL-31-342 Kraków, Poland*

(Received 17 December 2019; accepted 2 March 2020; published 31 March 2020)

We apply the k_T-factorization approach to the production of ϕ mesons in deep inelastic scattering. The helicity-conserving $\gamma^*(T, L) \to \phi$ impact factor is calculated for longitudinal and transverse photon polarization using ϕ meson distribution amplitudes. Different unintegrated gluon distributions are used in the calculations. The formalism for massless quarks/antiquarks gives too large transverse and longitudinal cross sections for photon virtualities below $Q^2 \sim 8$ GeV^2. We suggest how to improve the description of the HERA data by introducing effective strange-quark masses into the formalism. We derive the corresponding impact factor for a finite quark mass by comparing to the light-cone wave function representation used in previous k_T-factorization calculations and the color-dipole approaches. As a byproduct we present expressions for higher twist amplitudes as weighted integrals over the light-cone wave function. The quark mass $m_q \approx 0.5$ GeV allows to improve the description of both longitudinal and transverse cross sections down to $Q^2 \sim 4$ GeV^2 but this depends slightly on the renormalization scale used in the calculation. We also present the polarized cross section ratio σ_L/σ_T and the behavior of the total cross section $\sigma_{\rm tot} = \sigma_L + \sigma_T$ as a function of photon virtuality.

DOI: 10.1103/PhysRevD.101.054041

I. INTRODUCTION

The diffractive electroproduction of vector mesons, $\gamma^* p \to V p$, has attracted much attention at the HERA collider (for a review see e.g., Ref. [1]) and it is expected to be an important subject in future experiments e.g., at an electron-ion collider (EIC) [2]. In this work we are interested in the limit of large $\gamma^* p$ center-of-mass energy W, $s \equiv W^2 \gg Q^2 \gg \Lambda^2_{\rm QCD}$, which implies a small gluon longitudinal fraction $x = (Q^2 + m_V^2)/(W^2 + Q^2 - m_p^2) \sim Q^2/W^2$. In this kinematics, the photon virtuality Q^2 gives a handle on the dominant size of color dipoles in the $\gamma^* \to V$ transition and thus allows to study a transition from the hard, perturbative (small dipole), to the soft, nonperturbative (large dipole) regimes of scattering. In momentum space, the color-dipole approach has its correspondence in the k_T factorization, where the main ingredient is the unintegrated (transverse-momentum dependent) gluon distribution (UGD). At large photon virtualities the diffractive cross section is a sensitive probe of the proton UGD.

In the language of Regge theory, the dominant production mechanism at high energies is the t-channel Pomeron exchange [3]. One of the main results of the HERA accelerator was the observation that effectively, the intercept of the Pomeron depends on the hard scale of the process; see e.g., the review Ref. [1]. This behavior is indeed born out by the approaches in which the Pomeron exchange is modeled by a gluon ladder, such as the k_T-factorization approach used in this work, or the closely related color-dipole approach. For an application of the dipole approach to ϕ electroproduction, see e.g., Ref. [4].

The k_T-factorization formalism reviewed in Ref. [1] includes, besides the transverse momentum of gluons, the transverse momentum of the quark and antiquark in the vector meson as encoded in the light-cone wave function of the meson. This approach was used with some

*ad.bolognino@unical.it
†antoni.szczurek@ifj.edu.pl
‡wolfgang.schafer@ifj.edu.pl

success in Ref. [5]. At very large Q^2 one may expect, that the relative transverse motion of (anti)quarks in the bound state becomes negligible, and can be integrated out. Then, regarding the vector meson only a dependence on the longitudinal momentum fraction of quarks encoded in the distribution amplitudes (DAs) is left.

A quite general factorization formalism of vector-meson production in deep inelastic scattering was formulated in Refs. [6,7] and has been recently applied in Ref. [8] to the diffractive deep inelastic production of ρ mesons. While the production of longitudinal vector mesons involves the leading-twist DA, similar to the one introduced for other hadronic processes in Refs. [9–12], for transverse vector mesons higher twists are involved and the corresponding DAs studied in Ref. [13] are needed.

The recent analysis of helicity amplitudes for ρ^0 meson production [8] showed that this approach may be useful in testing UGDs.

In this paper, in order to test the formalism further, we wish to focus on and investigate the exclusive photoproduction of ϕ mesons:

$$\gamma^* p \to \phi p.$$

Corresponding experimental data were obtained by the H1 [14,15] and ZEUS [16] collaborations at HERA. In this paper we will show how the k_T-factorization approach of Ref. [17] matches to the higher-twist DA expansion, at least in the Wandzura-Wilczek (WW) approximation, where no explicit $q\bar{q}g$ contributions are included. Future applications at an EIC may require the inclusion of next-to-leading-order (NLO) contributions. Here the approach based on DAs has the advantage that for the case of collinear partons in the final state, the necessary techniques for the calculation of NLO impact factors are well advanced [18,19]. The first part of the paper is devoted to a summary of the theoretical framework of calculating the helicity amplitudes within the k_T-factorization approach. The second part shows the cross sections of the process and the effects due to UGDs and/or due to the strange-quark mass. Here we take advantage of the fact that we can rather straightforwardly derive the massive impact factor in the WW approximation from the light-cone wave function approach. As a byproduct we show how higher-twist DAs can be obtained from the light-cone wave functions which may also be interesting for the application of various light-cone models to other vector mesons.

A comparison with the H1 and ZEUS measurements are presented. The conclusion section closes our paper.

II. THEORETICAL FRAMEWORK

A. Helicity amplitudes $T_{\lambda_V \lambda_\gamma}$

In the high-energy regime, $s \equiv W^2 \gg Q^2 \gg \Lambda^2_{\rm QCD}$, which implies small $x = (Q^2 + m_V^2)/(W^2 + Q^2 - m_p^2) \sim Q^2/W^2$, the

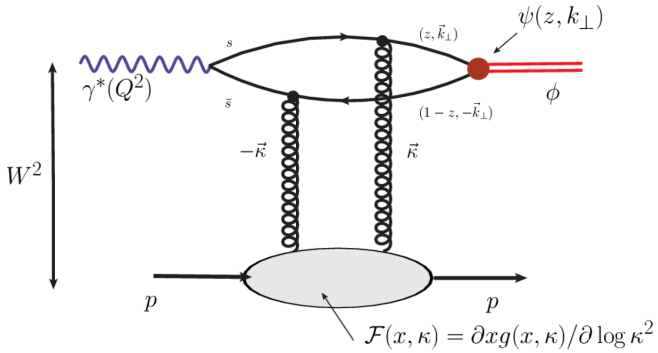

FIG. 1. A typical Feynman diagram for the $\gamma^* p \to \phi p$ forward amplitude, at cm energy W. The t-channel gluons carry transverse momenta $\pm\boldsymbol{\kappa}$. The transverse momentum of quarks $\pm\boldsymbol{k}$ is integrated out in the approach based on distribution amplitudes.

forward helicity amplitude $T_{\lambda_V \lambda_\gamma}$ can be expressed, in the k_T factorization, as the convolution of the $\gamma^* \to V$ impact factor (IF), $\Phi^{\gamma^* \to V}_{\lambda_V, \lambda_\gamma}(\boldsymbol{\kappa}^2, Q^2)$, with the UGD, $\mathcal{F}(x, \boldsymbol{\kappa}^2)$. Here, $\pm\boldsymbol{\kappa}$ is the transverse momentum (in the $\gamma^* p$ frame) carried by the exchanged gluon (see Fig. 1).

Our normalization of the impact factor is chosen, such that the forward amplitude for the $\gamma^* p \to V p$ process reads

$$\Im m T_{\lambda_V \lambda_\gamma}(s, Q^2) = s \int \frac{d^2\boldsymbol{\kappa}}{(\boldsymbol{\kappa}^2)^2} \Phi^{\gamma^* \to V}_{\lambda_V, \lambda_\gamma}(\boldsymbol{\kappa}^2, Q^2) \mathcal{F}(x, \boldsymbol{\kappa}^2). \quad (1)$$

Here, the UGD is related to the collinear gluon parton distribution as

$$x g(x, \mu^2) = \int^{\mu^2} \frac{d\boldsymbol{\kappa}^2}{\boldsymbol{\kappa}^2} \mathcal{F}(x, \boldsymbol{\kappa}^2). \quad (2)$$

We now turn to the two different approaches to the impact factors which we want to compare in this work.

B. Distribution amplitude expansion

We start with the scheme based on the collinear factorization of the meson structure which was worked out in Refs. [6,7] and was used recently for ρ-meson electroproduction in Ref. [8]. This approach starts from the observation, that at large Q^2 the transverse internal motion of partons in the meson can be neglected.

The longitudinal impact factor is expressed in terms of the standard twist-2 distribution amplitude. In the normalization adopted by us, the IF for the $L \to L$ transition reads

$$\Phi^{\gamma^* \to V}_{0,0}(\boldsymbol{\kappa}^2, Q^2) = \frac{4\pi\alpha_S(\mu_r^2) e_q \sqrt{4\pi\alpha_{\rm em}} f_V}{N_c Q} \int_0^1 dy\, \varphi_1(y; \mu^2) \times \left(\frac{\alpha}{\alpha + y\bar{y}} \right), \quad (3)$$

where $\alpha = \boldsymbol{\kappa}^2/Q^2$, y is the fraction of the mesons' light-cone plus momentum carried by the quark, $\bar{y} = 1 - y$, and $\varphi_1(y;\mu^2)$ is the twist-2 DA. It is normalized as

$$\int_0^1 dy\, \varphi_1(y;\mu^2) = 1 \tag{4}$$

and we recall its asymptotic form

$$\varphi_1(y;\mu^2) \overset{\mu^2\to\infty}{\longrightarrow} \varphi_1^{as}(y) = 6y\bar{y}. \tag{5}$$

The expression for the transverse case is

$$\begin{aligned}\Phi_{+,+}^{\gamma^*\to V}(\boldsymbol{\kappa}^2, Q^2) = {}& \frac{2\pi\alpha_S(\mu_r^2)e_q\sqrt{4\pi\alpha_{\rm em}}f_V m_V}{N_c Q^2}\times\left\{\int_0^1 dy\,\frac{\alpha(\alpha+2y\bar{y})}{y\bar{y}(\alpha+y\bar{y})^2}[(y-\bar{y})\varphi_1^T(y;\mu^2)+\varphi_A^T(y;\mu^2)]\right.\\
&-\int_0^1 dy_2\int_0^{y_2} dy_1\,\frac{y_1\bar{y}_1\alpha}{\alpha+y_1\bar{y}_1}\times\left[\frac{2-N_c/C_F}{\alpha(y_1+\bar{y}_2)+y_1\bar{y}_2}-\frac{N_c/C_F}{y_2\alpha+y_1(y_2-y_1)}\right]M(y_1,y_2;\mu^2)\\
&+\int_0^1 dy_2\int_0^{y_2} dy_1\left[\frac{2+N_c/C_F}{\bar{y}_1}+\frac{y_1}{\alpha+y_1\bar{y}_1}\left(\frac{(2-N_c/C_F)y_1\alpha}{\alpha(y_1+\bar{y}_2)+y_1\bar{y}_2}-2\right)\right.\\
&\left.\left.-\frac{N_c}{C_F}\frac{(y_2-y_1)\bar{y}_2}{\bar{y}_1}\frac{1}{\alpha\bar{y}_1+(y_2-y_1)\bar{y}_2}\right]S(y_1,y_2;\mu^2)\right\},\end{aligned} \tag{6}$$

where

$$C_F = \frac{N_c^2-1}{2N_c}, \tag{7}$$

$$B(y_1,y_2;\mu^2) = -5040y_1\bar{y}_2(y_1-\bar{y}_2)(y_2-y_1), \tag{8}$$

$$\begin{aligned}D(y_1,y_2;\mu^2) = {}& -360y_1\bar{y}_2(y_2-y_1)\\
&\times\left(1+\frac{\omega_{\{1,0\}}^A(\mu^2)}{2}(7(y_2-y_1)-3)\right),\end{aligned} \tag{9}$$

and where the three-body DAs read

$$\begin{aligned}M(y_1,y_2;\mu^2) = {}& \zeta_{3V}^V(\mu^2)B(y_1,y_2;\mu^2)\\
&-\zeta_{3V}^A(\mu^2)D(y_1,y_2;\mu^2),\end{aligned} \tag{10}$$

$$\begin{aligned}S(y_1,y_2;\mu^2) = {}& \zeta_{3V}^V(\mu^2)B(y_1,y_2;\mu^2)\\
&+\zeta_{3V}^A(\mu^2)D(y_1,y_2;\mu^2)\end{aligned} \tag{11}$$

with the dimensionless coupling constants $\zeta_{3V}^V(\mu^2)$ and $\zeta_{3V}^A(\mu^2)$ defined as

$$\zeta_{3V}^V(\mu^2) = \frac{f_{3V}^V(\mu^2)}{f_V}, \qquad \zeta_{3V}^A(\mu^2) = \frac{f_{3V}^A(\mu^2)}{f_V}. \tag{12}$$

The dependence on the factorization scale μ^2 can be determined from evolution equations [13] (see also Appendix B in Ref. [7]), with the initial condition at a renormalization scale $\mu_0 = 1$ GeV.

The DAs $\varphi_1^T(y;\mu^2)$ and $\varphi_A^T(y;\mu^2)$ in Eq. (6) encompass both genuine twist-3 and WW contributions[1] [13].

While the distribution amplitude for the pion has been frequently discussed, there are only a few studies on the case of the ϕ meson; see e.g., Ref. [20]. Here we follow Ref. [8] and truncate the Gegenbauer expansion of the DA at the second order

$$\phi_1(y,\mu^2) = 6y\bar{y}\left(1+a_2(\mu^2)\frac{3}{2}(5(y-\bar{y})^2-1)\right). \tag{13}$$

We will neglect a_2 below. A very small value for a_2 was found e.g., in Refs. [13,20]. Also a small a_2 is obtained from the light-cone wave function discussed below. In the distribution amplitude formalism one often includes the QCD evolution of $\phi_1(y,\mu^2)$. However, for the ϕ meson where the initial distribution amplitude is already very close to the asymptotic one the evolution can be safely neglected.

C. Light-cone wave function approach

In the light-cone k_T-factorization approach, the calculation proceeds in a slightly different way. Here one calculates the amplitude for the $\gamma^* p \to q\bar{q}p$ diffractive process and projects the final state $q\bar{q}$ pair onto the vector-meson state. We treat the ϕ meson as a pure $s\bar{s}$ state. The meson of momentum $P = (P_+, m_\phi^2/(2P_+), \mathbf{0})$ is described by the $s\bar{s}$ light-cone wave function (LCWF) as

[1]Genuine terms are related to $B(y_1,y_2;\mu^2)$ and $D(y_1,y_2;\mu^2)$; WW contributions, instead, are those obtained in the approximation in which $B(y_1,y_2;\mu^2) = D(y_1,y_2;\mu^2) = 0$. For their expressions in this last case see Eq. (9) in Refs. [7,8].

$$|\phi, P_+, \lambda_V\rangle = \int \frac{dyd^2\boldsymbol{k}}{y\bar{y}16\pi^3}\Psi^{(\lambda_V)}_{\lambda\bar{\lambda}}(y,\boldsymbol{k})|s(yP_+,\boldsymbol{k},\lambda) \times \bar{s}(\bar{y}P_+,-\boldsymbol{k},\bar{\lambda})\rangle + \cdots \tag{14}$$

The amplitude for diffractive vector-meson production then takes the form

$$\Im m T_{\lambda_V,\lambda_\gamma}(s,Q^2) = s\int \frac{dyd^2\boldsymbol{k}}{y\bar{y}16\pi^3}\sum_{\lambda\bar{\lambda}}\mathcal{M}^{(\lambda_\gamma)}_{\lambda\bar{\lambda}}(\gamma^* p\to s\bar{s}p)\Psi^{(\lambda_V)*}_{\lambda\bar{\lambda}}(y,\boldsymbol{k}). \tag{15}$$

The explicit expressions for the diffractive amplitudes can be found in Ref. [1]. Here we are interested only in the forward scattering limit of vanishing transverse momentum transfer, where only the helicity-conserving amplitudes with $\lambda_V = \lambda_\gamma$ contribute.

We can easily read off the following expressions for the impact factors of interest. The $L \to L$ IF reads

$$\Phi^{\gamma^*\to\phi}_{0,0}(\boldsymbol{\kappa}^2,Q^2) = \sqrt{4\pi\alpha_{\rm em}}e_q 8\pi\alpha_S(\mu_r^2)Q\int\frac{dyd^2\boldsymbol{k}}{\sqrt{y\bar{y}}16\pi^3}I_0(\boldsymbol{k},\boldsymbol{\kappa}) \times y\bar{y}\{\Psi^{(0)*}_{+-}(y,\boldsymbol{k})+\Psi^{(0)*}_{-+}(y,\boldsymbol{k})\}. \tag{16}$$

For the $T \to T$ IF we obtain

$$\Phi^{\gamma^*\to\phi}_{\pm,\pm}(\boldsymbol{\kappa}^2,Q^2) = \sqrt{4\pi\alpha_{\rm em}}e_q 4\pi\alpha_S(\mu_r^2)\int\frac{dyd^2\boldsymbol{k}}{\sqrt{y\bar{y}}16\pi^3}\times[(\boldsymbol{e}(\pm)\cdot\boldsymbol{I}_1(\boldsymbol{k},\boldsymbol{\kappa}))\{(y-\bar{y})(\Psi^{(\pm)*}_{+-}(y,\boldsymbol{k})+\Psi^{(\pm)*}_{-+}(y,\boldsymbol{k})) + \Psi^{(\pm)*}_{+-}(y,\boldsymbol{k})-\Psi^{(\pm)*}_{-+}(y,\boldsymbol{k})\}+\sqrt{2}m_q I_0(\boldsymbol{k},\boldsymbol{\kappa})\Psi^{(\pm)*}_{++}(y,\boldsymbol{k})]. \tag{17}$$

Here

$$I_0(\boldsymbol{k},\boldsymbol{\kappa}) = \frac{1}{\boldsymbol{k}^2+\varepsilon^2}-\frac{1}{(\boldsymbol{k}+\boldsymbol{\kappa})^2+\varepsilon^2},$$
$$\boldsymbol{I}_1(\boldsymbol{k},\boldsymbol{\kappa}) = \frac{\boldsymbol{k}}{\boldsymbol{k}^2+\varepsilon^2}-\frac{\boldsymbol{k}+\boldsymbol{\kappa}}{(\boldsymbol{k}+\boldsymbol{\kappa})^2+\varepsilon^2}, \tag{18}$$

and $\varepsilon^2 = m_q^2 + y\bar{y}Q^2$. We now want to compare these results with the twist expansion approach presented in the previous subsections. To this end, we should expand the impact factors around the limit of collinear kinematics for the $q\bar{q}$ pair. While an analogous expansion around the small-$\boldsymbol{\kappa}$ limit, has been discussed in great detail, the analogous comparison to leading- and higher-twist distribution amplitudes is up to now missing.

Expanding in $\boldsymbol{k}^2/(\boldsymbol{\kappa}^2+\varepsilon^2) \ll 1$, we obtain

$$I_0(\boldsymbol{k},\boldsymbol{\kappa}) \approx \frac{1}{\varepsilon^2}-\frac{1}{\boldsymbol{\kappa}^2+\varepsilon^2} = \frac{\boldsymbol{\kappa}^2}{\varepsilon^2(\boldsymbol{\kappa}^2+\varepsilon^2)}, \tag{19}$$

and

$$\boldsymbol{I}_1(\boldsymbol{k},\boldsymbol{\kappa}) \approx \boldsymbol{k}\frac{\boldsymbol{\kappa}^2}{\varepsilon^2(\boldsymbol{\kappa}^2+\varepsilon^2)}+\frac{2(\boldsymbol{k}\cdot\boldsymbol{\kappa})\boldsymbol{\kappa}}{(\boldsymbol{\kappa}^2+\varepsilon^2)^2}\to\frac{\boldsymbol{\kappa}^2(\boldsymbol{\kappa}^2+2\varepsilon^2)}{\varepsilon^2(\boldsymbol{\kappa}^2+\varepsilon^2)^2}\boldsymbol{k}, \tag{20}$$

where we performed the azimuthal average in the last step. Inserting the expanded I_0 into the IF for the $L \to L$ transition, we find

$$\Phi^{\gamma^*\to\phi}_{0,0}(\boldsymbol{\kappa}^2,Q^2) = \sqrt{4\pi\alpha_{\rm em}}e_q 8\pi\alpha_S(\mu_r^2)Q\int_0^1 dy\, y\bar{y}\frac{\boldsymbol{\kappa}^2}{\varepsilon^2(\boldsymbol{\kappa}^2+\varepsilon^2)}\times\frac{1}{\sqrt{y\bar{y}}}\int\frac{d^2\boldsymbol{k}}{16\pi^3}\{\Psi^{(0)*}_{+-}(y,\boldsymbol{k})+\Psi^{(0)*}_{-+}(y,\boldsymbol{k})\}\theta(\mu^2-\boldsymbol{k}^2)$$
$$= \sqrt{4\pi\alpha_{\rm em}}e_q\frac{4\pi\alpha_S(\mu_r^2)f_V}{N_c Q}\int_0^1 dy\frac{y\bar{y}}{(y\bar{y}+\tau)}\frac{\alpha}{(\alpha+y\bar{y}+\tau)}\varphi_1(y,\mu^2). \tag{21}$$

Here we introduced the variables $\alpha = \boldsymbol{\kappa}^2/Q^2$ and $\tau = m_q^2/Q^2$. We see that we have obtained a generalization of the impact factor of Eq. (3) including a finite quark mass. The helicity combination of the LCWF which appears under the $\boldsymbol{k}$ integral gives rise to the leading-twist distribution amplitude of the longitudinally polarized vector meson, defined following the rules of Ref. [11] as

$$f_V\varphi_1(y,\mu_0^2) = \frac{2N_c}{\sqrt{y\bar{y}}}\int\frac{d^2\boldsymbol{k}}{16\pi^3}\theta(\mu_0^2-\boldsymbol{k}^2)\{\Psi^{(0)*}_{+-}(y,\boldsymbol{k})+\Psi^{(0)*}_{-+}(y,\boldsymbol{k})\}. \tag{22}$$

The scale μ^2 in Eq. (21) must be chosen such that the small-$\boldsymbol{k}$ expansion is valid, i.e., $\mu^2 \sim (Q^2+m_\phi^2)/4$.

We can now follow a similar strategy for the transverse IF. To that end we introduce the following representations of the higher-twist DAs:

$$f_V\varphi_1^T(y,\mu_0^2) = \frac{2N_c}{\sqrt{y\bar{y}}}\int\frac{d^2\boldsymbol{k}}{16\pi^3}\theta(\mu_0^2-\boldsymbol{k}^2)(\boldsymbol{e}(\pm)\cdot\boldsymbol{k})\{\Psi_{+-}^{(\pm)*}(y,\boldsymbol{k})+\Psi_{-+}^{(\pm)*}(y,\boldsymbol{k})\},$$
$$f_V\varphi_A^T(y,\mu_0^2) = \frac{2N_c}{\sqrt{y\bar{y}}}\int\frac{d^2\boldsymbol{k}}{16\pi^3}\theta(\mu_0^2-\boldsymbol{k}^2)(\boldsymbol{e}(\pm)\cdot\boldsymbol{k})\{\Psi_{+-}^{(\pm)*}(y,\boldsymbol{k})-\Psi_{-+}^{(\pm)*}(y,\boldsymbol{k})\},$$
$$f_V\varphi_m(y,\mu_0^2) = \frac{2N_c}{\sqrt{y\bar{y}}}\int\frac{d^2\boldsymbol{k}}{16\pi^3}\theta(\mu_0^2-\boldsymbol{k}^2)\sqrt{2}m_q\Psi_{++}^{(\pm)*}(z,\boldsymbol{k}). \tag{23}$$

We notice, that

$$\int_0^1 dy\,\varphi(y,\mu_0^2)=1, \qquad \int_0^1 dy\,\varphi_1^T(y,\mu_0^2)=0. \tag{24}$$

The transverse IF that we derive is again a generalization of Eq. (6) to finite quark mass and reads

$$\Phi_{\pm,\pm}^{\gamma\to\phi}(\boldsymbol{\kappa}^2,Q^2) = \sqrt{4\pi\alpha_{\rm em}}e_q\frac{2\pi\alpha_S(\mu_r^2)f_V}{N_cQ^2}\int_0^1\frac{dy}{y\bar{y}+\tau}\left\{\frac{\alpha(\alpha+2y\bar{y}+2\tau)}{(\alpha+y\bar{y}+\tau)^2}\right.$$
$$\left.\times((y-\bar{y})\varphi_1^T(y,\mu^2)+\varphi_1^A(y,\mu^2))+\frac{\alpha}{\alpha+y\bar{y}+\tau}\varphi_m(y,\mu^2)\right\}. \tag{25}$$

We realize that up to the DA φ_m, which vanishes in the massless limit, the structure of the IF is exactly the same as for the one of Eq. (6) neglecting the so-called genuine three-particle distributions. The latter obviously can appear only at the level of the $q\bar{q}g$ Fock state.

We now wish to give some explicit expressions for the DAs in question. To this end, we use the $V\to q\bar{q}$ vertex from Ref. [1], where the ϕ meson is treated as a pure S-wave bound state of a strange quark and antiquark. For the relevant combinations of light-cone wave functions we obtain in the case of the longitudinally polarized vector meson

$$\Psi_{+-}^{(0)*}(y,\boldsymbol{k})+\Psi_{-+}^{(0)*}(y,\boldsymbol{k}) = -4M\sqrt{y\bar{y}}\left\{1+\frac{(y-\bar{y})^2}{4y\bar{y}}\frac{2m_q}{M+2m_q}\right\}\psi(y,\boldsymbol{k}). \tag{26}$$

The radial wave function $\psi(y,\boldsymbol{k})$ is normalized as

$$N_c\int\frac{dyd^2\boldsymbol{k}}{y\bar{y}16\pi^3}2M^2|\psi(y,\boldsymbol{k})|^2=1. \tag{27}$$

Above $M^2=(\boldsymbol{k}^2+m_q^2)/(y\bar{y})$ is the invariant mass of the $s\bar{s}$ system. We can now express the leading-twist DA through the radial WF as

$$f_V\varphi_1(y,\mu_0^2) = \frac{N_c}{2\pi^2}\int_0^{\mu_0^2}d\boldsymbol{k}^2M\left\{1+\frac{(y-\bar{y})^2}{4y\bar{y}}\frac{2m_q}{M+2m_q}\right\}\times\psi(y,\boldsymbol{k}). \tag{28}$$

Now, for the higher-twist DAs of the transversely polarized vector meson, we obtain

$$f_V\varphi_1^T(y,\mu_0^2) = (y-\bar{y})\frac{N_c}{8\pi^2}\int_0^{\mu_0^2}d\boldsymbol{k}^2\,\boldsymbol{k}^2\frac{M}{M+2m_q}\frac{\psi(y,\boldsymbol{k})}{y\bar{y}},$$
$$f_V\varphi_A^T(y,\mu_0^2) = \frac{N_c}{4\pi^2}\int_0^{\mu_0^2}d\boldsymbol{k}^2\,\boldsymbol{k}^2\frac{\psi(y,\boldsymbol{k})}{y\bar{y}},$$
$$f_V\varphi_m(y,\mu_0^2) = m_q^2\frac{N_c}{4\pi^2}\int_0^{\mu_0^2}d\boldsymbol{k}^2\left\{1+\frac{\boldsymbol{k}^2}{m_q(M+2m_q)}\right\}\times\frac{\psi(y,\boldsymbol{k})}{y\bar{y}}. \tag{29}$$

D. Characteristic parameters

Typical constants for ϕ mesons, entering the DAs and IFs, used in numerical computations, are provided in Tables I and II.

TABLE I. Experimental value of the coupling to the vector current [21] (first row) and the couplings entering the vector-meson DAs at the scale $\mu_0=1$ GeV.

V	ϕ
f_V [GeV]	0.254
ζ_{3V}^A	0.032
ζ_{3V}^V	0.013
$\omega_{1,0}^A$	−2.1
$\omega_{1,0}^V$	28/3

TABLE II. Decay constants obtained from Eq. (12).

V	ϕ
$m_V f_{3V}^A$ [GeV^2]	3.37×10^{-3}
$m_V f_{3V}^V$ [GeV^2]	5.26×10^{-3}

E. Cross section and diffraction slope

The imaginary part of the amplitude in Eq. (1) which enters the expression of the cross section for transverse and longitudinal polarization, can be written as

$$\sigma_L(\gamma^* p \to Vp) = \frac{1}{16\pi b(Q^2)} \left| \frac{T_{00}(s,Q^2)}{W^2} \right|^2, \quad (30)$$

$$\sigma_T(\gamma^* p \to Vp) = \frac{1}{16\pi b(Q^2)} \left| \frac{T_{11}(s,Q^2)}{W^2} \right|^2, \quad (31)$$

where $b(Q^2)$ is the diffraction slope which depends on the virtuality of the photon and it is parametrized in the present analysis as follows [22]:

$$b(Q^2) = \beta_0 - \beta_1 \log\left[\frac{Q^2 + m_\phi^2}{m_{J/\psi}^2}\right] + \frac{\beta_2}{Q^2 + m_\phi^2}, \quad (32)$$

with $\beta_0 = 7.0$ GeV^{-2}, $\beta_1 = 1.1$ GeV^{-2} and $\beta_2 = 1.1$.

In Fig. 2 we show a plot of our parametrization of the diffractive slope. The full cross section is a sum of longitudinal and transverse components, and it reads

$$\sigma_{\rm tot}(\gamma^* p \to Vp) = \sigma_T + \epsilon \sigma_L, \quad (33)$$

where $\epsilon \approx 1$ due to HERA kinematics.

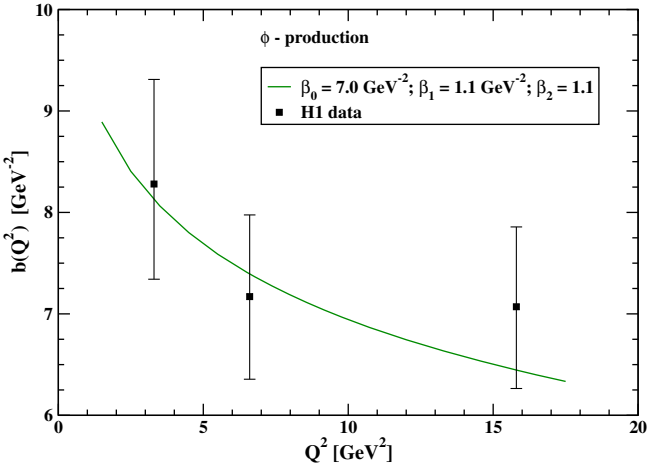

FIG. 2. Q^2 dependence of the diffraction slope $b(Q^2)$ for ϕ-meson production in the $\gamma^* p \to \phi p$ reaction. Due to the high uncertainty of the experimental data, we keep the standard choices for the β_0, β_1 and β_2 parameters from Ref. [22] for all our results.

F. Unintegrated gluon distributions

Before turning to the numerical results, let us briefly review the salient properties of the unintegrated gluon distributions used in this work.

(1) Ivanov-Nikolaev UGD:

The UGD proposed in Ref. [17] probes different regions of the transverse momentum. In the large-κ region, DGLAP parametrizations for $g(x,\kappa^2)$ are used. Moreover, for the extrapolation of the hard gluon densities to small κ^2, an ansatz is made [23]. The gluon density at small κ^2 is endowed with a nonperturbative soft part, according to the color-dipole phenomenology. This model of UGD has the following form:

$$\mathcal{F}(x,\kappa^2) = \mathcal{F}_{\rm soft}^{(B)}(x,\kappa^2)\frac{\kappa_s^2}{\kappa^2+\kappa_s^2} + \mathcal{F}_{\rm hard}(x,\kappa^2)\frac{\kappa^2}{\kappa^2+\kappa_h^2}, \quad (34)$$

where $\kappa_s^2 = 3$ GeV^2 and $\kappa_h^2 = [1 + 0.047\log^2(1/x)]^{1/2}$ GeV^2.

The soft term reads

$$\mathcal{F}_{\rm soft}^{(B)}(x,\kappa^2) = a_{\rm soft} C_F N_c \frac{\alpha_S(\kappa^2)}{\pi}\left(\frac{\kappa^2}{\kappa^2+\mu_{\rm soft}^2}\right)^2 V_{\rm N}(\kappa), \quad (35)$$

where $C_F = \frac{N_c^2-1}{2N_c}$ and $\mu_{\rm soft} = 0.1$ GeV. The parameter $a_{\rm soft} = 2$ gives a measure of how important the soft part is compared to the hard one. On the other hand, the hard component is

$$\mathcal{F}_{\rm hard}(x,\kappa^2) = \mathcal{F}_{\rm pt}^{(B)}(\kappa^2)\frac{\mathcal{F}_{\rm pt}(x,Q_c^2)}{\mathcal{F}_{\rm pt}^{(B)}(Q_c^2)}\theta(Q_c^2-\kappa^2) + \mathcal{F}_{\rm pt}(x,\kappa^2)\theta(\kappa^2-Q_c^2), \quad (36)$$

where $\mathcal{F}_{\rm pt}(x,\kappa^2)$ is related to the standard gluon parton distribution. We refer to Ref. [17] for insights about the expressions of the vertex function $V_{\rm N}(\kappa)$ and of $\mathcal{F}_{\rm pt}^{(B)}(\kappa^2)$ as well as about discussions of the parameter of this model. Another important feature of this UGD is given by the choice of the coupling constant. The infrared freezing of the strong coupling at leading order is imposed by fixing $\Lambda_{\rm QCD} = 200$ MeV:

$$\alpha_S(\mu^2) = \min\left\{0.82, \frac{4\pi}{\beta_0 \log(\frac{\mu^2}{\Lambda_{\rm QCD}^2})}\right\}. \quad (37)$$

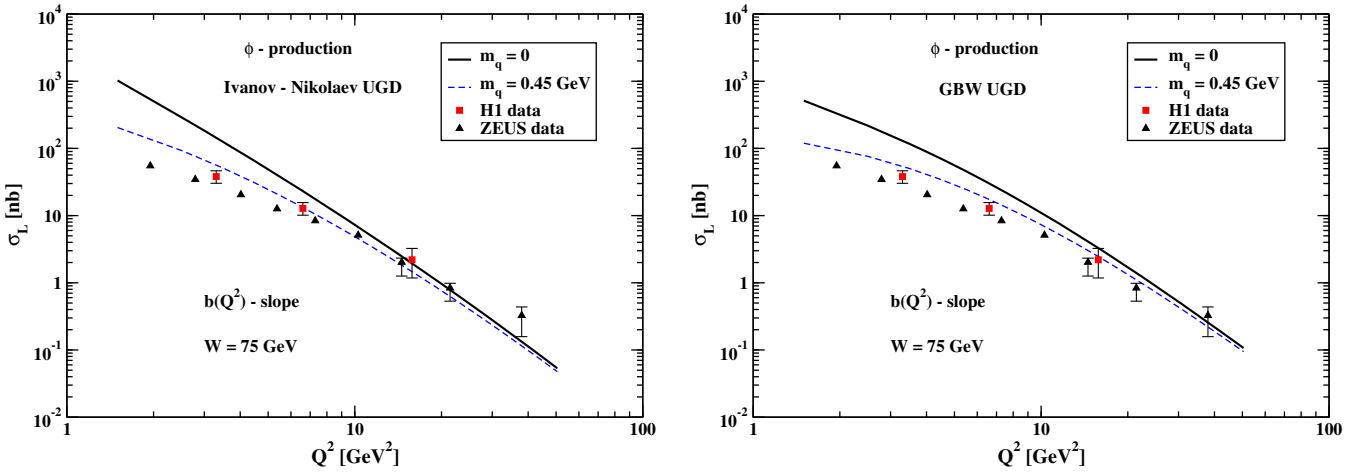

FIG. 3. Q^2 dependence of the longitudinal cross section σ_L of ϕ-meson production, at $W = 75$ GeV, in comparison with experimental data of the H1 [15] and ZEUS [16] collaborations. The result is obtained within the k_T factorization using the Ivanov-Nikolaev UGD model (left panel) and the GBW one (right panel). The solid lines are for the case when the strange-quark mass is neglected and the dashed lines are for the strange-quark mass fixed at $m_q = 0.45$ GeV. In both cases, the asymptotic DA is used.

(2) Golec-Biernat–Wüsthoff (GBW) UGD:

This UGD parametrization comes from the effective dipole cross section $\hat{\sigma}(x, r)$ for the scattering of a $q\bar{q}$ pair off a nucleon [24],

$$\hat{\sigma}(x, r^2) = \sigma_0 \left\{ 1 - \exp\left(-\frac{r^2}{4R_0^2(x)} \right) \right\}, \tag{38}$$

through a reverse Fourier transform of the expression

$$\sigma_0 \left\{ 1 - \exp\left(-\frac{r^2}{4R_0^2(x)} \right) \right\} = \frac{2\pi}{N_c} \int \frac{d^2\kappa}{\kappa^4} \alpha_S \mathcal{F}(x, \kappa^2)(1 - \exp(i\vec{\kappa} \cdot \vec{r})) \times (1 - \exp(-i\vec{\kappa} \cdot \vec{r})), \tag{39}$$

$$\frac{4\pi}{N_c} \alpha_S \mathcal{F}(x, \kappa^2) = \kappa^4 \sigma_0 \frac{R_0^2(x)}{2\pi} e^{-\kappa^2 R_0^2(x)}, \tag{40}$$

with

$$R_0^2(x) = \frac{1}{\text{GeV}^2} \left(\frac{x}{x_0} \right)^{\lambda_p} \tag{41}$$

and the following values:

$$\sigma_0 = 23.03\,\text{mb}, \quad \lambda_p = 0.288, \quad x_0 = 3.04 \times 10^{-4}. \tag{42}$$

The normalization σ_0 and the parameters x_0 and λ_p of $R_0^2(x)$ have been determined by a global fit to $F_2(x, Q^2)$ in the region $x < 0.01$.

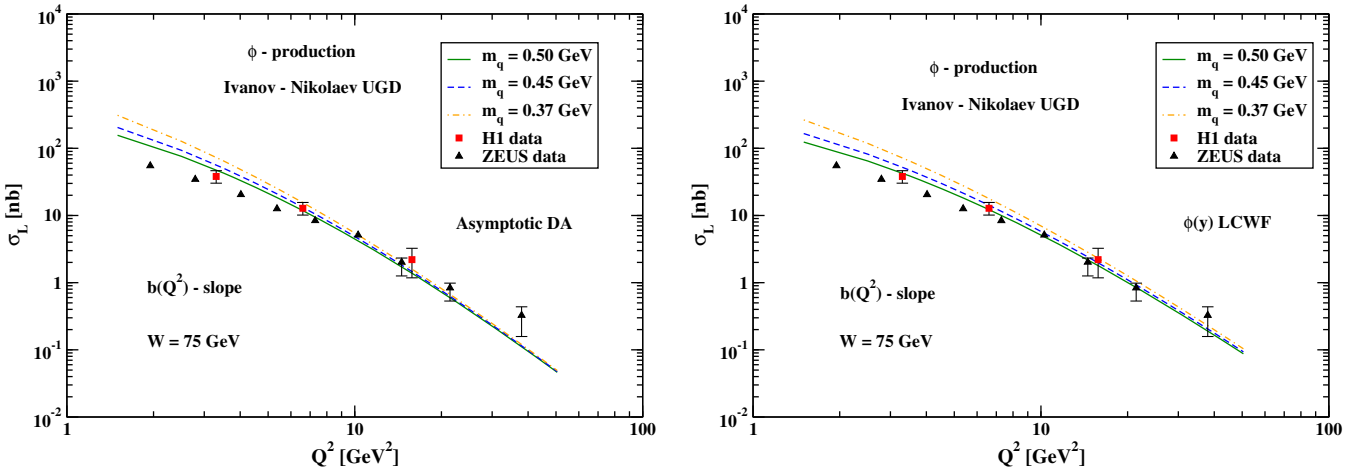

FIG. 4. σ_L for the asymptotic DA (left panel) and for the LCWF DA (right panel). Results for three different strange-quark-mass values are shown. Predictions are given using the Ivanov-Nikolaev UGD model.

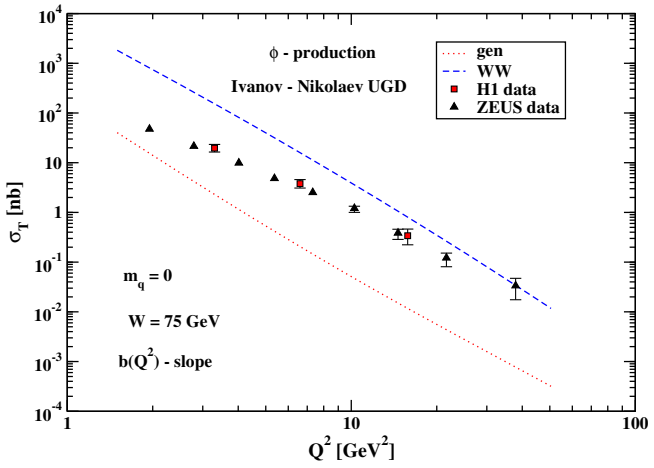

FIG. 5. Q^2 dependence of the transverse cross section σ_T neglecting the quark mass m_q. The WW and the genuine three-parton contributions are shown separately.

III. NUMERICAL RESULTS

In what follows we present theoretical predictions adopting two different UGD models:

(1) The Ivanov-Nikolaev parametrization, endowed with soft and hard components to probe both large and small transverse momentum regions (see Ref. [17] for further details).

(2) The model provided by Golec-Biernat and Wüsthoff, which derives from the dipole cross section for the scattering of a $q\bar{q}$ pair off a nucleon [24].

We start by calculating the longitudinal cross section using the formalism described in the previous section. In Fig. 3 we show the results of our calculation for the Ivanov-Nikolaev (left panel) and GBW (right panel) UGDs. In order to get these predictions, below we always use for the renormalization scale in the strong coupling $\mu_r^2 = Q^2$. As far as the scale dependence in the DA is concerned, in Fig. 3, the asymptotic DA has been used. This calculation has been obtained for $W = 75$ GeV. We observe that the cross sections obtained for massless strange quarks (black solid line) overestimate the experimental cross section below $Q^2 < 10$ GeV^2. This is very different for ρ^0 production to be discussed elsewhere. In both cases we also present our results when using quarks/antiquarks with effective masses. The quark mass enters the calculation through the parameter $\tau = m_q^2/Q^2$ in the relevant impact factors; see Eq. (21) and Eq. (25). Including a finite quark mass, a good description of the experimental data is obtained for both the Ivanov-Nikolaev and GBW UGDs.

How much the cross section depends on the quark mass is shown in Fig. 4 for the asymptotic (left panel) and LCWF (right panel) DAs, respectively. The best description of the data is obtained with $m_q = 0.5$ GeV. A similar result was found in Ref. [5] within the k_T-factorization approach with a Gaussian $s\bar{s}$ light-cone wave function for the ϕ meson. The preferred quark mass very much resembles the typical value expected for a constituent quark. We note in passing, that for the light mesons ρ and ω, a similar approach [25] suggests $m_{u,d} \sim 300$ MeV. Now we pass to the transverse cross section as a function of photon virtuality.

In Fig. 5 we show the cross sections for the Wandzura-Wilczek and genuine three-parton contributions. In this calculation massless quarks were used. We observe that the transverse cross section for the genuine three-parton contribution is rather small. However, the WW contribution for massless quarks, similarly as for the longitudinal cross section, overpredicts the H1 and ZEUS data. Can this be

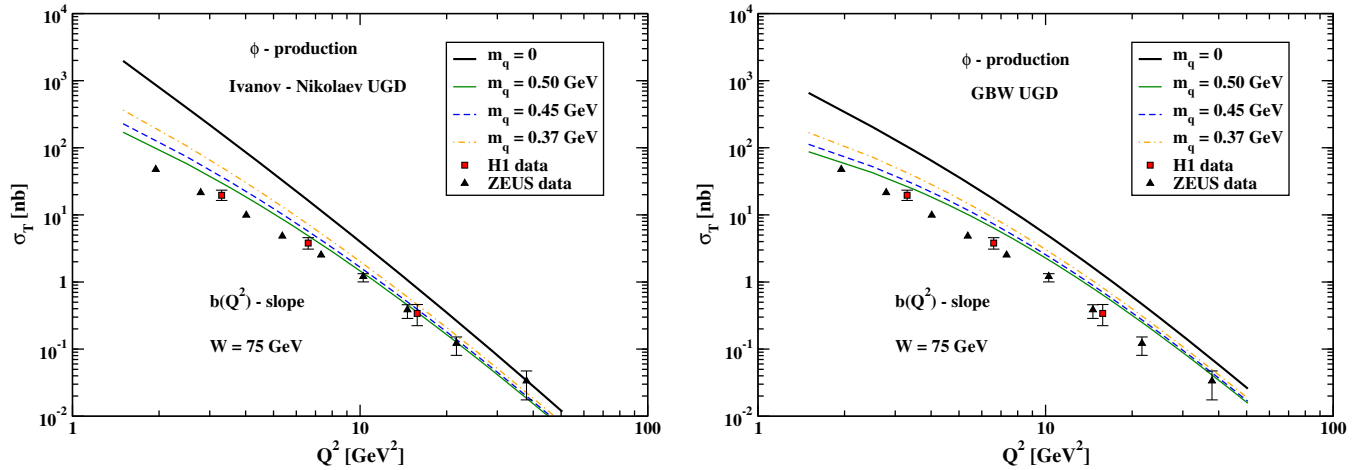

FIG. 6. Q^2 dependence of the transverse cross section σ_T for the ϕ-meson production in the $\gamma^* p \to \phi p$ reaction, at $W = 75$ GeV, in comparison with the H1 [15] and ZEUS [16] experimental data. The result is obtained within the k_T factorization using the Ivanov-Nikolaev UGD model (left panel) and the GBW one (right panel). The thick solid line is for the case when the strange-quark mass is neglected. The thin lines show the results for the three different values of the strange-quark mass. In both cases, the curves were obtained with the asymptotic choice of the DA.

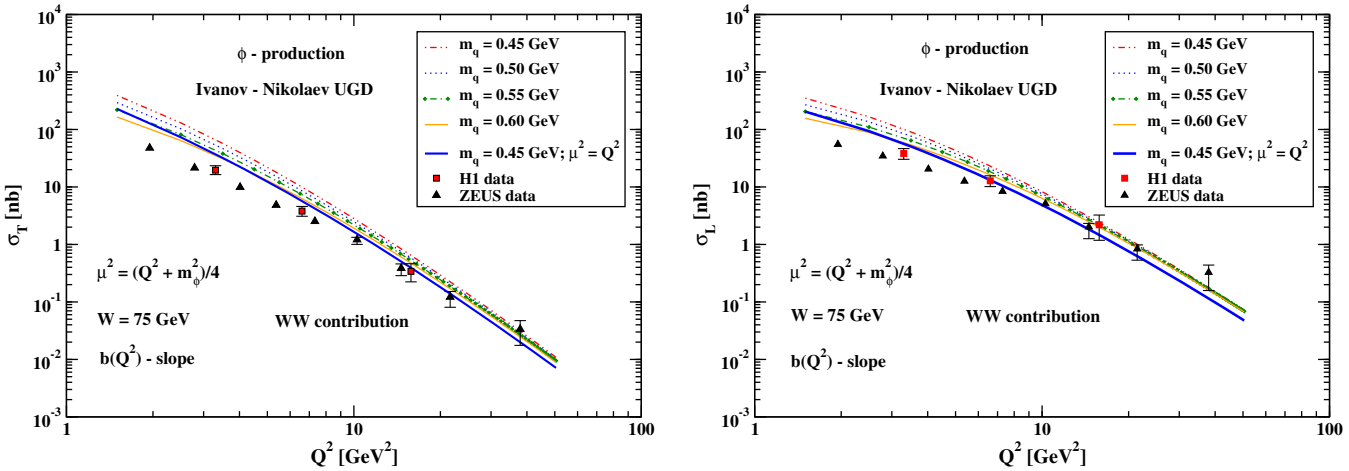

FIG. 7. Q^2 dependence of the transverse (left panel) and longitudinal (right panel) cross section for the $\mu_r^2 = (\frac{Q^2+m_\phi^2}{4})$. We show results for different strange quark masses specified in the figure. For comparison by the thick line we present for comparison our standard choice $\mu_r^2 = Q^2$.

explained as due to the mass effect discussed in the previous section?

In Fig. 6 we show how the WW contribution changes when including the mass effect discussed in the previous section. The inclusion of the mass effect improves the description of the H1 and ZEUS experimental transverse cross section. The description is, however, not perfect. In Fig. 6 we present a similar result for both UGD models. Unlike for the longitudinal cross section, here the GBW overpredicts the experimental data in the whole range of virtuality, while the Ivanov-Nikolaev model only overpredicts at smaller Q^2 values. A reasonable result is obtained when including the mass effect.

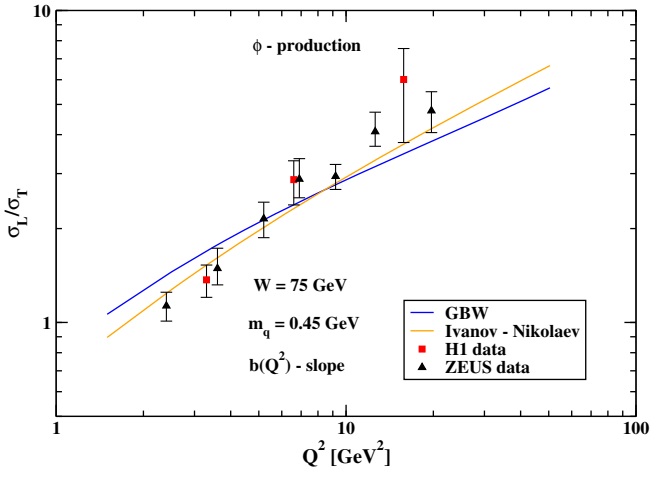

FIG. 8. Q^2 dependence of cross section ratio σ_L/σ_T for the ϕ-meson production in the $\gamma^* p \to \phi p$ reaction, at $W = 75$ GeV, in comparison with experimental data of the H1 [15] and ZEUS [16] collaborations. The prediction is performed in the k_T-factorization approach, using both UGD models: the Ivanov-Nikolaev model and the GBW one. The strange-quark mass is fixed here at $m_q = 0.45$ GeV.

As for any truncated pQCD calculations, here the cross section also depends on the choice of the renormalization scale. For the vector-meson production sometimes one uses the renormalization scale $\mu_r^2 = (Q^2 + m_\phi^2)/4$ [1]. As shown in Fig. 7 this choice leads to a larger cross section than for $\mu_r^2 = Q^2$, at least for the same effective quark mass. Then the calculated cross section is somewhat above the H1 and ZEUS experimental data. To improve the agreement with the data one can increase m_s as is shown in Fig. 7. Then $m_s \sim 0.6$ GeV would lead to a better agreement with the experimental data. This mass is a bit larger than the one used in Ref. [5] where the effects of the transverse motion of quarks and a dynamical choice of the renormalization scale were included explicitly.

We also wish to show results for the σ_L/σ_T ratio (see Fig. 8) as a function of photon virtuality Q^2 for the Ivanov-Nikolaev and GBW UGDs. In this calculation the quark mass was fixed for $m_q = 0.45$ GeV. The Ivanov-Nikolaev UGD better describes the H1 and ZEUS data.

How much does the ratio depend on the effective quark mass parameter? This is shown in Fig. 9. The ratio is much less sensitive to the quark mass than the polarized cross sections σ_L and/or σ_T separately. So the extraction of the mass parameter from the normalized cross section is preferred.

Now we shall show the total cross section $\sigma_{\rm tot}$ as a function of virtuality. In Fig. 10 we show both the longitudinal and transverse components as well as their sum. The transverse cross section is somewhat steeper (falls faster with virtuality) than the longitudinal one. The comparison with the HERA data is presented in Fig. 11. The GBW UGD better describes the experimental data at small photon virtualities. There seems to be a small

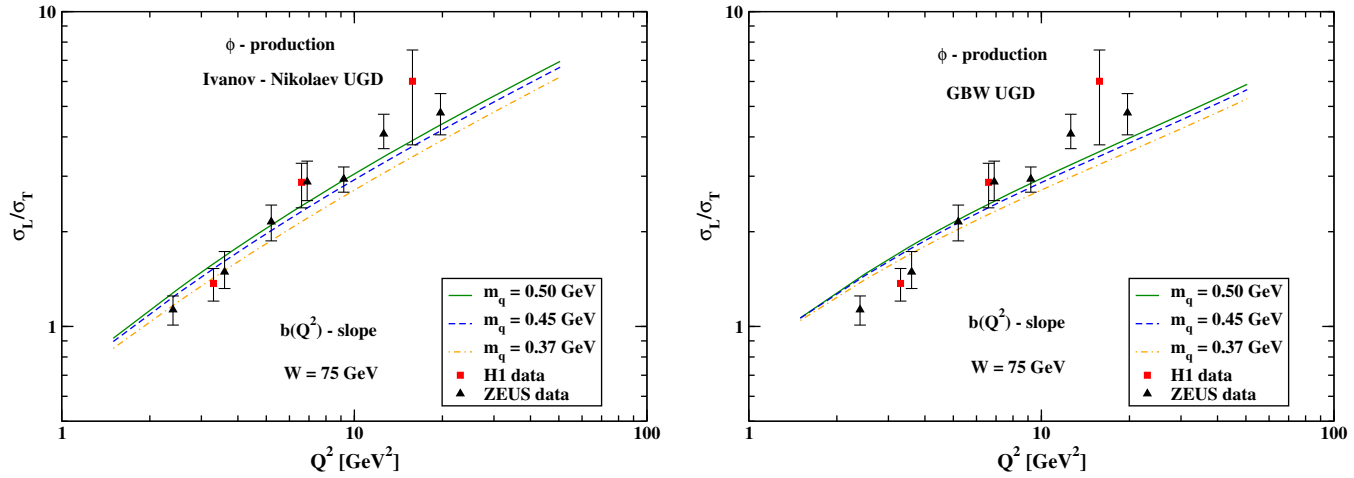

FIG. 9. Q^2 dependence of the cross section ratio σ_L/σ_T for three different quark-mass values m_q using the Ivanov-Nikolaev (left panel) and the GBW (right panel) UGDs.

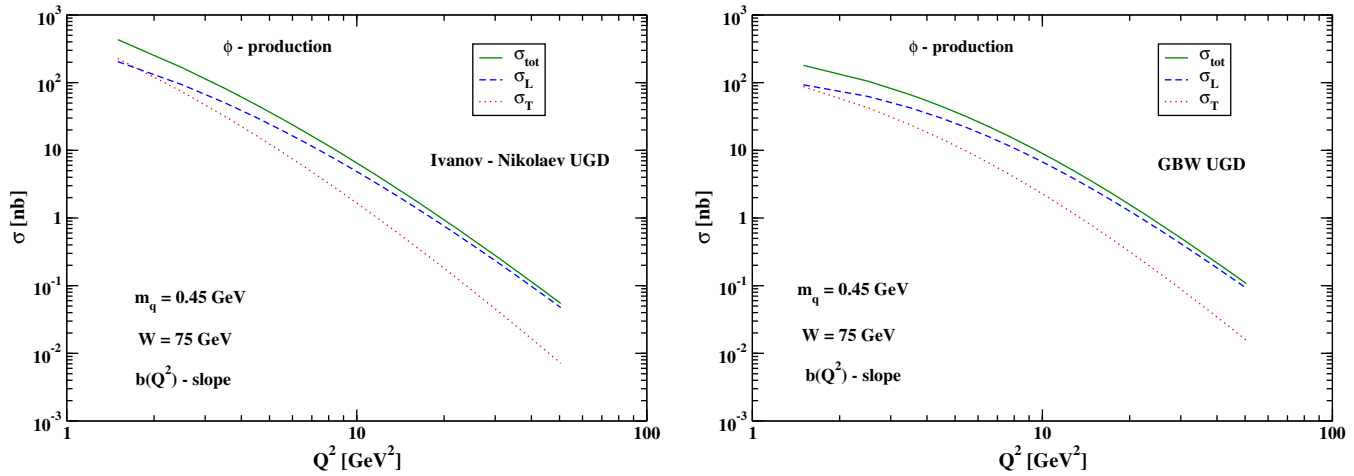

FIG. 10. Longitudinal, transverse and total cross sections as functions of Q^2 using the Ivanov-Nikolaev (left panel) and the GBW (right panel) UGDs.

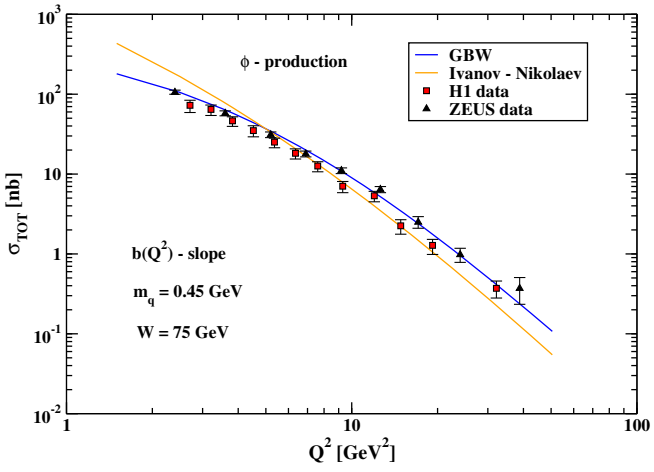

FIG. 11. Q^2 dependence of total cross section $\sigma_{\rm tot}$ at $W = 75$ GeV for both UGD models in comparison with the H1 [15] and ZEUS [16] experimental data.

inconsistency between the H1 and ZEUS data at larger virtualities.

So far we did not consider skewness effects and the real part of the $\gamma^* p \to \phi p$ amplitude. Both these corrections can be calculated from the energy dependence of the forward amplitude. Defining

$$\Delta_{\mathbf{IP}} = \frac{\partial \log(\Im m T_{\lambda_V \lambda_\gamma}(s, Q^2)/s)}{\partial \log(1/x)}, \tag{43}$$

we can calculate the real part from

$$\rho = \frac{\Re e T_{\lambda_V \lambda_\gamma}(s, Q^2)}{\Im m T_{\lambda_V \lambda_\gamma}(s, Q^2)} = \tan\left(\frac{\pi \Delta_{\mathbf{IP}}}{2}\right). \tag{44}$$

The skewness correction is obtained from multiplying the forward amplitude by the factor [26]

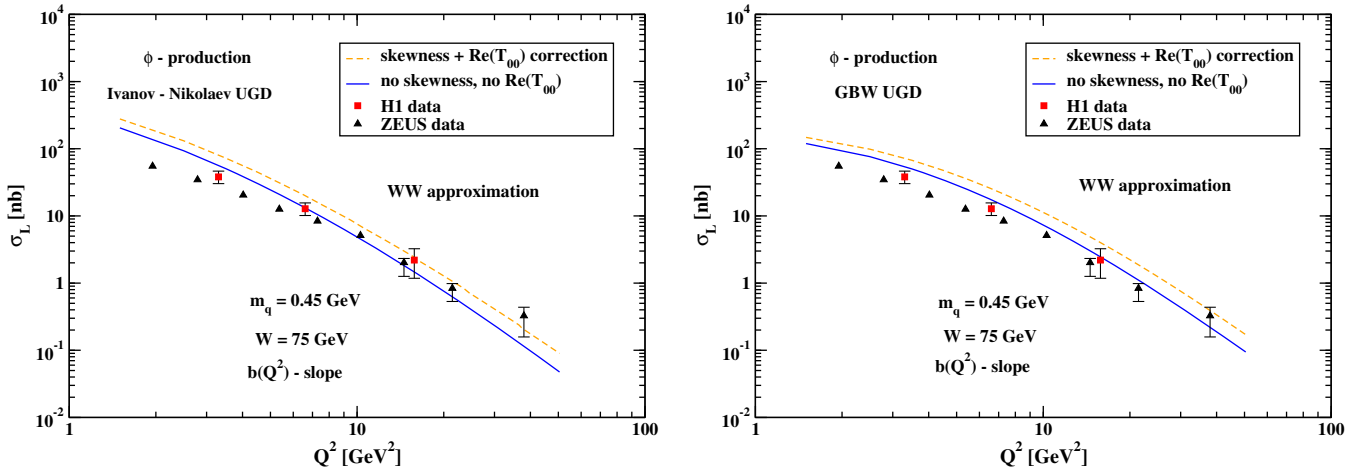

FIG. 12. An estimation of the skewness effects and the real part of the amplitude for the longitudinal cross section σ_L calculated in the WW approximation using the Ivanov-Nikolaev (left panel) and GBW (right panel) UGDs.

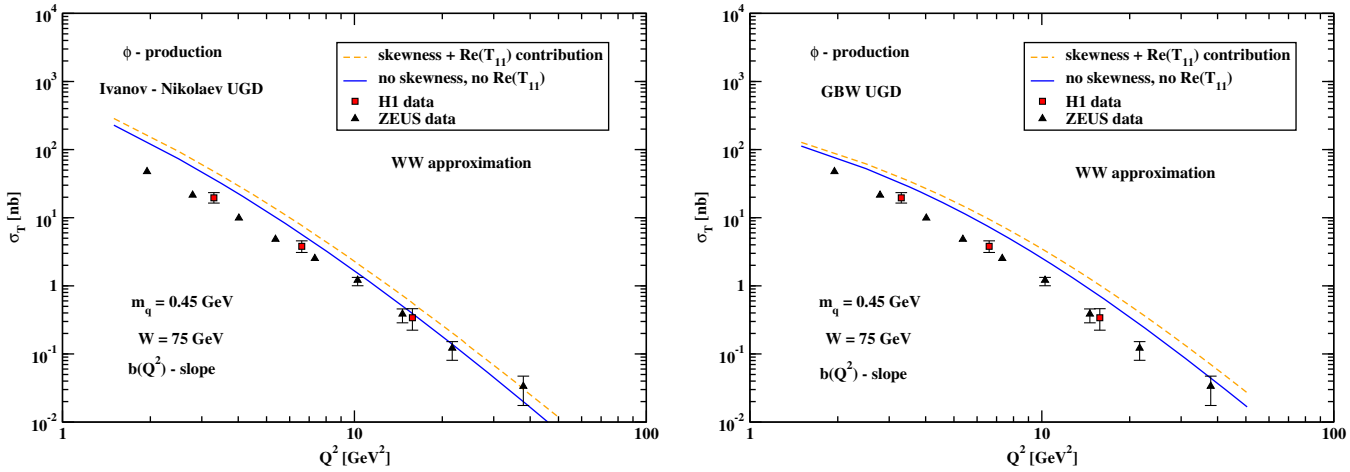

FIG. 13. An estimation of the skewness effects and the real part of the amplitude for the transverse cross section σ_T calculated in the WW approximation using the Ivanov-Nikolaev (left panel) and GBW (right panel) UGDs.

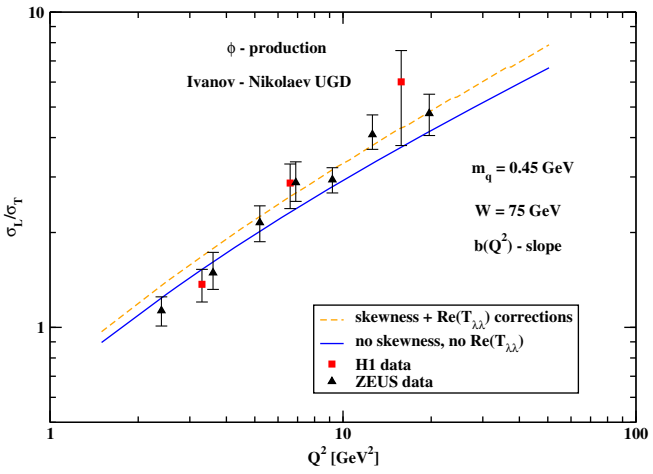

FIG. 14. An estimation of the skewness effects and the real part of the amplitude are shown for the cross section ratio σ_L/σ_T through the Ivanov-Nikolaev UGD.

$$R_{\rm skewed} = \frac{2^{2\Delta_{\rm IP}+3}}{\sqrt{\pi}} \cdot \frac{\Gamma(\Delta_{\rm IP}+5/2)}{\Gamma(\Delta_{\rm IP}+4)}. \tag{45}$$

Now we wish to show our estimates of these corrections. We show results for the longitudinal (Fig. 12) and transverse (Fig. 13) components separately. The effect is not too big but cannot be neglected. The effect of the skewness is much larger than the effect of the inclusion of the real part. We observe that the effect of the skewness does not cancel in the σ_L/σ_T ratio as can be seen in Fig. 14.

IV. CONCLUSIONS

In the present paper we have used a recently formulated hybrid formalism for the production of ϕ mesons in the $\gamma^* p \to \phi p$ reaction using unintegrated gluon distributions and meson distribution amplitudes. In this formalism the $\gamma^* \to \phi$ impact factor is calculated in collinear factorization

using (collinear) distribution amplitudes. So far this formalism was used only for massless quarks/antiquarks (e.g., for ρ^0 meson production). Both twist-2 and twist-3 contributions are included. The impact factor for the $p \to p$ transition is expressed in terms of UGDs. Two different UGD models have been used.

We have shown that for massless quarks the genuine three-parton contribution is more than an order of magnitude smaller than the WW one. Therefore in this paper we have concentrated on the WW component.

We have observed a too quick rise of the cross section when going to smaller photon virtualities compared to the experimental data measured by the H1 and ZEUS collaborations at HERA. This was attributed to the massless quarks/antiquarks. We have proposed how to include effective quark masses into the formalism. Corresponding distribution amplitudes were calculated and have been used in the present approach. With the effective quark mass $m_q \sim 0.5$ GeV a good description of the H1 and ZEUS data has been achieved for the Ivanov-Nikolaev and GBW UGDs down to $Q^2 \sim 4$ GeV^2. This value of the strange-quark mass is similar to the one found in Ref. [5], where the k_T-factorization formalism with the $s\bar{s}$ light-cone wave function of the ϕ meson was used for real photoproduction.

We also have estimated the skewness effect which turned out to be not too big but not negligible. We have shown some residual effects of the skewness for the ratio of longitudinal-to-transverse cross sections.

ACKNOWLEDGMENTS

A. D. B, thanks the University of Calabria and Instituto Nazionale di Fisica Nucleare for support of her stay in Kraków. We are indebted to Alessandro Papa for a discussion. This study was partially supported by the Polish National Science Center Grant No. UMO-2018/31/B/ST2/03537 and by the Center for Innovation and Transfer of Natural Sciences and Engineering Knowledge in Rzeszów.

[1] I. P. Ivanov, N. N. Nikolaev, and A. A. Savin, Phys. Part. Nucl. **37**, 1 (2006).
[2] A. Accardi *et al.*, Eur. Phys. J. A **52**, 268 (2016).
[3] S. Donnachie, H. G. Dosch, O. Nachtmann, and P. Landshoff, Cambridge Monogr. Part. Phys., Nucl. Phys., Cosmol. **19**, 1 (2002).
[4] J. R. Forshaw, R. Sandapen, and G. Shaw, Phys. Rev. D **69**, 094013 (2004).
[5] A. Cisek, W. Schäfer, and A. Szczurek, Phys. Lett. B **690**, 168 (2010).
[6] I. V. Anikin, D. Yu. Ivanov, B. Pire, L. Szymanowski, and S. Wallon, Nucl. Phys. **B828**, 1 (2010).
[7] I. V. Anikin, A. Besse, D. Yu. Ivanov, B. Pire, L. Szymanowski, and S. Wallon, Phys. Rev. D **84**, 054004 (2011).
[8] A. D. Bolognino, F. G. Celiberto, D. Yu. Ivanov, and A. Papa, Eur. Phys. J. C **78**, 1023 (2018).
[9] A. V. Radyushkin, arXiv:hep-ph/0410276; A. V. Efremov and A. V. Radyushkin, Teor. Mat. Fiz. **42**, 147 (1980) [Theor. Math. Phys. **42**, 97 (1980)]; Phys. Lett. B **94**, 245 (1980).
[10] G. P. Lepage and S. J. Brodsky, Phys. Lett. B **87**, 359 (1979).
[11] G. P. Lepage and S. J. Brodsky, Phys. Rev. D **22**, 2157 (1980).
[12] V. L. Chernyak and A. R. Zhitnitsky, Phys. Rep. **112**, 173 (1984).
[13] P. Ball, V. M. Braun, Y. Koike, and K. Tanaka, Nucl. Phys. **B529**, 323 (1998).
[14] C. Adloff *et al.* (H1 Collaboration), Phys. Lett. B **483**, 360 (2000).
[15] F. D. Aaron *et al.* (H1 Collaboration), J. High Energy Phys. 05 (2010) 032.
[16] S. Chekanov *et al.* (ZEUS collaboration), Nucl. Phys. **B718** (2005).
[17] I. P. Ivanov and N. N. Nikolaev, Phys. Rev. D **65**, 054004 (2002).
[18] D. Yu. Ivanov, M. I. Kotsky, and A. Papa, Eur. Phys. J. C **38**, 195 (2004).
[19] D. Yu. Ivanov and A. Papa, Nucl. Phys. **B732**, 183 (2006).
[20] F. Gao, L. Chang, Y. X. Liu, C. D. Roberts, and S. M. Schmidt, Phys. Rev. D **90**, 014011 (2014).
[21] M. Tanabashi *et al.* (Particle Data Group), Phys. Rev. D **98**, 030001 (2018).
[22] J. Nemchik, N. N. Nikolaev, E. Predazzi, B. G. Zakharov, and V. R. Zoller, Zh. Eksp. Teor. Fiz. **113**, 1930 (1998) [J. Exp. Theor. Phys. **86**, 1054 (1998)].
[23] N. N. Nikolaev and B. G. Zakharov, Phys. Lett. B **332**, 177 (1994); Z. Phys. C **53**, 331 (1992).
[24] K. J. Golec-Biernat and M. Wüsthoff, Phys. Rev. D **59**, 014017 (1998).
[25] A. Cisek, P. Lebiedowicz, W. Schäfer, and A. Szczurek, Phys. Rev. D **83**, 114004 (2011).
[26] A. G. Shuvaev, K. J. Golec-Biernat, A. D. Martin, and M. G. Ryskin, Phys. Rev. D **60**, 014015 (1999).